Available online at www.sciencedirect.com
SCIENCE DIRECT
Journal of Photochemistry and Photobiology B: Biology 84 (2006) 46–55
Journal of Photochemistry and Photobiology B:Biology
www.elsevier.com/locate/jphotobiol

Photocount distribution of photons emitted from three sites of a human body

Roeland Van Wijk [a,b,*], Eduard P.A. Van Wijk [b], Rajendra P. Bajpai [b,c]

[a] *Faculty of Biology, Utrecht University, 3501 TB Utrecht, The Netherlands*
[b] *International Institute of Biophysics, Raketenstation Hombroich, Kapellener Strasse, D-41472 Neuss, Germany*
[c] *Sophisticated Analytical Instruments Facility, North Eastern Hill University, Shillong 793022, India*

Received 16 September 2005; received in revised form 15 December 2005; accepted 19 January 2006
Available online 7 March 2006

Abstract

Spontaneous photon emission from 30 sites on the skin of a live human subject is measured at different times and on different days. Signals from three representative sites of low, intermediate and high intensities are selected for further analysis. Fluctuations in these signals are measured by the probabilities of detecting different numbers of photons in a bin. The probabilities have non-classical features and are well described by the signal in a quantum squeezed state of photons. Measurements with bins of three sizes yield same values of three parameters of the squeezed state. A procedure for making correction due to background noise is developed. The correction changes the parameters of the quantum state. The new state appears more like a coherent state of photons.

Keywords: Weak photon emission; Human skin; Photocount distribution; Squeezed state; Background correction

1. Introduction

Novel macroscopic photonic imaging technologies in combination with emerging data analysis provide researchers with several techniques to visualize biological processes. These technologies grow into an important tool in biomedical research [1]. The whole body imaging technology exploring ultra-weak light, spontaneously emitted from humans without any artificially induced external excitation, has been receiving relatively less attention [2].

Ultra weak photon emission is generated during metabolic processes. The various characteristics of the emitted photon signal, e.g., shape, spectral decomposition and photocount statistics constitute biological information. Emission is incorporated in various biochemical processes, especially in radical reactions associated with the production of reactive oxygen species, and many pioneering studies have suggested the potential usefulness of non-invasive monitoring of oxidative metabolism and oxidative damage to tissue [3–6].

The quantum stochastic nature of such field reflects the properties of the elementary processes of excitation and photon emission. The semi-classical theory of light describes two models of such field: (a) a chaotic field that accompanies a Gaussian intensity fluctuation from independent radiators; (b) a coherent field that accompanies a probabilistic intensity fluctuation. A biological system is a highly integrated organization from the subcellular level to the macroscopic (anatomic) level with complex regulation circuitry through elemental interactions. It has been argued that the excitation process in metabolically active complex organisms does not originate from statistically independent events. The radiation field emitted by biochemical processes underlying metabolism fluctuates in intensity as a result of interplay among elementary bio-

* Corresponding author. Present address: Department of Molecular and Cellular Biology, University of Utrecht, P.O. Box 80.056, 3508 TR Utrecht, The Netherlands. Tel.: +31 345 570080; fax: +31 345 570110.
E-mail address: meluna.wijk@wxs.nl (R. Van Wijk).

1011-1344/$ - see front matter © 2006 Elsevier B.V. All rights reserved.
doi:10.1016/j.jphotobiol.2006.01.010

chemical reactions in the physiological state [7]. The intensity fluctuations carry information on the regulatory processes and are expected to be different from chaotic light. The Q values of the sets of photocount measurements in photon signals emitted by quasi-stable non-human living systems suggest that low-level photon signals are in quantum squeezed states [8–10].

Recent studies in human photon emission imaging demonstrate spontaneous ultra-weak photon emission distribution patterns from larger anatomic sites using CCD imaging [11,12]. To unravel the information provided by the fluctuations in photon counts in anatomic locations with different intensities, we have used a set up that uses a sensitive photomultiplier tube cooled to −25 °C for photon detection and permits manipulation of the measuring area in three directions over the human body [13–15].

Fluctuations in a signal of constant average intensity are measured by photocount distribution that gives the probabilities of detecting different number of photons in the signal. Photocount distribution at low intensities of around 0.1 counts in a measuring interval is very effective in discriminating between classical and quantum signals. Photocount distribution at moderate intensity of a few counts in a measuring interval can provide information about the possible quantum state of the signal. The information is obtained by comparing observed photocount distribution with photocount distribution calculated in the expected state. The expected state contains a few unknown parameters, whose values give the information. The expected state has to be guessed from the other properties of the signal. Our guess of the quantum state of photon signal emitted by living systems is a squeezed state. A squeezed state is specified by two arbitrary complex parameters. The average intensity of the signal is constant if parameters are time independent but can show decay if parameters are time dependent. The parameters of the squeezed state can be determined in a signal of constant average intensity by measuring photocount distribution. These determinations were made in samples of three lichen species [8–10]. The different determinations in a sample yield nearly same values of squeezed state parameters. The squeezed state parameters appear measurable in living samples only. Similar determinations in a photon signal of comparable intensity emitted by a light emitting diode (LED) yield different values of squeezed state parameters. A good determination of squeezed state parameters is obtained with signal strength of a few counts in the measuring interval and a stable photocount distribution. Photocount distribution in a signal of few counts becomes stable with ten thousands or more data points. Both conditions were met in measurements with lichen samples. These conditions are difficult to impose in measurements with human subjects. We have restricted the investigation of fluctuations to 200 s periods. We have measured photon intensity at 30 sites distributed throughout the body of a human subject and studied the variation in the intensity of emitted photons. The investigation of fluctuations at all 30 sites would have been too strenuous on the subject. We have restricted the study of intensity fluctuations to three anatomical locations with different intensities.

2. Materials and methods

2.1. Dark room and photomultiplier device

A special dark room of dimensions of 2 m × 1.5 m × 2 m (inner size) was used for the recording apparatus. The temperature of the dark room averaged 20 °C. Subjects were measured supine or sitting. A photomultiplier (EMI 9235 QB, selected for low noise; Electron Tubes Limited, Ruislip, England) can be manipulated in three directions [13–15]. The photomultiplier tube contains a 52 mm diameter window for recording and has a spectral sensitivity range of 200–650 nm. The photomultiplier was mounted in a sealed housing under vacuum with a quartz window and was maintained at −25 °C to reduce dark current (background noise). Dark current was measured weekly as well as before and after each experiment. During the experimental period the average and standard error of background values was 5.1 ± 0.1 cps (or counts per second).

An additional 7 cm broad ring at the front port of the photomultiplier tube allows the measurement of 9 cm diameter skin area at a fixed distance of 7 cm. The front ring is vented inside avoiding the condensation of moisture at the quartz window.

2.2. Recording of spontaneous emission

The subject was asked to remain in door and avoid bright sunlight for 2 h prior to a measurement. The subject was then dark adapted for 1 h prior to recording of photon emission. This procedure was adopted to eliminate contribution to photon emission arising from the previous exposure to light and was based on our previous studies [14–16].

Subsequently, the subject was positioned in the dark room. The photomultiplier tube was placed directly above the skin for recording, the ring at the front port of the photomultiplier touching the skin.

In multi-site recording the duration of each recording was 2 min with emission counts grouped for each 1 s.

For photocount distribution, the palm of left hand, forehead, and upper part of frontal upper leg were selected for recording. Photocount distribution analysis was carried out with recordings of 20,000 contiguous intervals of 50, 100 and 200 ms duration. Details are stated in Section 3.

2.3. Data analysis

Statistical analysis of photon count data was performed with Statistica 6.1, and squeezed state parameters were determined by the minimization program in Mathcad 2000 Professional.

3. Results and discussion

3.1. Topographical intensity variation of spontaneous photon emission

Fig. 1 illustrates locations on the skin selected for recording of photon emission. The recording of anatomic locations began at the ventral part of the body and from top to bottom locations; it was then continued dorsally in the reverse direction. Total duration of measurement was approximately 70 min. Fig. 2 presents the emissions of the same subject at different times of the day. Relative variation of intensity of photon emission at various locations of an individual was not much different at different times. It perhaps, indicates that broad features of relative intensity at various locations are specific to an individual. The thorax–abdomen region produces signal of the lowest intensity. In contrast, the upper extremities emit most intense signals. The other locations have intermediate intensities.

Three skin areas of the subject were selected for determining photocount distribution of the emission. The selected body sites were palm of the left hand (Ha-p-l), forehead (Fhd), and upper part of frontal upper right leg (Up-A-r). The intensities of photon emission at these locations were significantly different: the intensity was highest in the emission from the palm, intermediate from the forehead and the lowest from the upper leg.

3.2. Statistical properties of emitted photons

Photocount distribution was measured in photon signals from the three body sites. Its measurement had two contradictory requirements: a large number of points in a set of

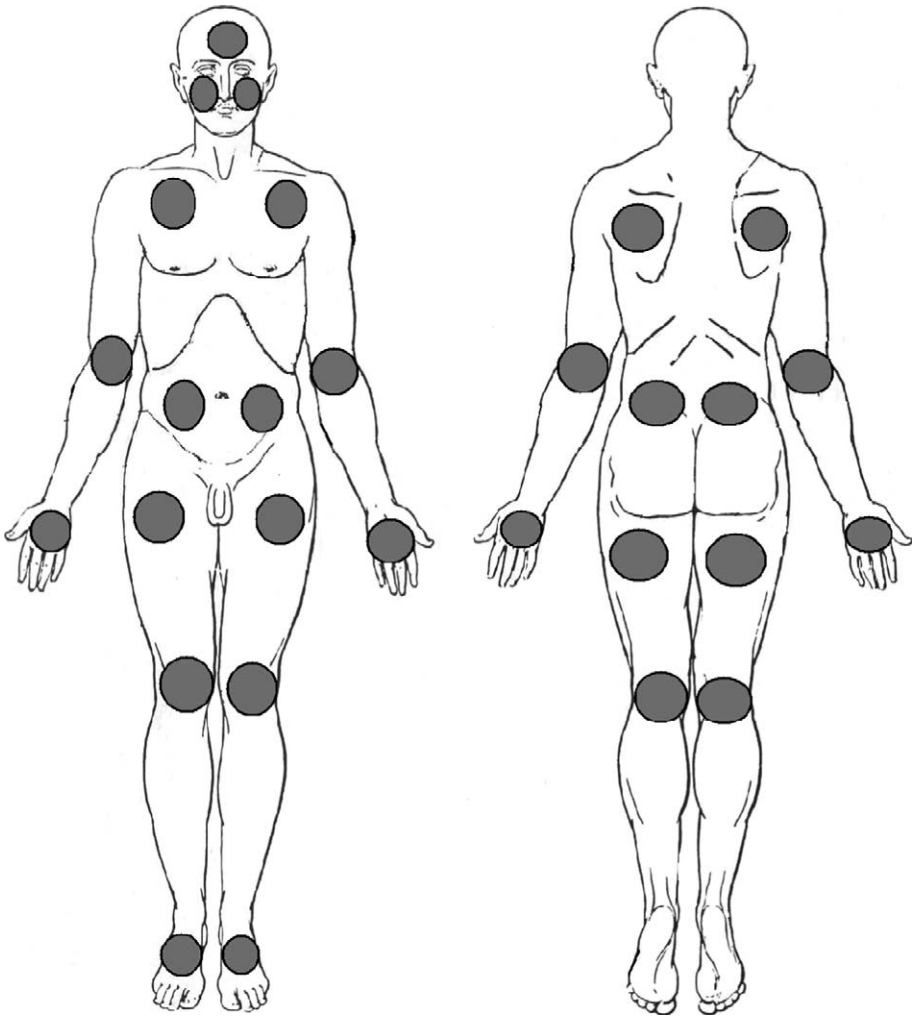

Fig. 1. Map of locations for measurement of spontaneous photon emission over the anterior (left figure) and posterior (right figure) of the human body: the body locations on the left (l) and right (r) side were abbreviated as follows: forehead (FHD), cheek (Chk), thorax-anterior (Th-A), thorax-posterior, scapulae (Th-P), abdomen-anterior (Ab-A), abdomen-posterior, kidneys (Ab-P), elbow-anterior (El-A), elbow-posterior (El-P), hand palm (Ha-p), hand dorsal (Ha-d), upper leg-anterior (Up-A), upper leg-posterior (Up-P), knee (Kne), hollow of knee (HKn), and foot frontal (Fof). The front of the body (anterior) was measured first, starting at the forehead and then downwards at each level the photomultiplier moved from left to right. After the subject turned the dorsal part (posterior) of the body was measured, starting at the legs and then upwards.

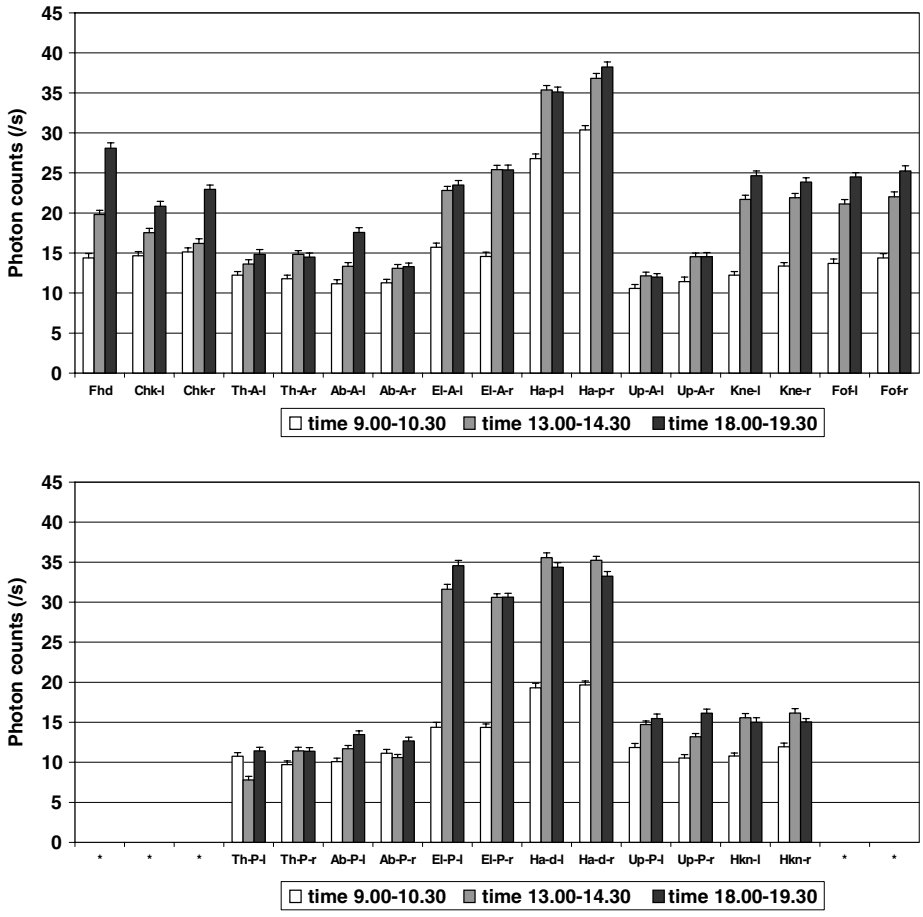

Fig. 2. Multi-site spontaneous photon emission of the anterior (upper panel) and posterior (lower panel) part of a subject on three occasions during a day: each body site was recorded for 120 s. Mean background value was 5.8 ± 0.4 cps. The latter data include mean dark current of the photomultiplier of 4.9 ± 0.4 cps. For abbreviated anatomical sites, see Fig. 1.

measurements and short time in completing the set of measurements. A large number of points ensures better determination of various probabilities while a short duration is needed to minimize changes in the physiological state of the subject. A photocount distribution will measure fluctuations only if the state of the signal remains unchanged during measurements. We opted for duration of 200 s to complete a set of measurements in contiguous bins. Three sets of measurements were made with bin size (or dwell time) = 50, 100 and 200 ms. The sets contained 4000, 2000 and 1000 data points, respectively. Five independent recordings were accomplished at the three body locations and for background noise with shutter closed.

Statistical analysis of each set of data was made independently. The first step of the analysis was to calculate first four statistical moments, mean, variance, skewness, and kurtosis. The values of these moments were almost identical in five independent measurements, which indicate that detected signals have stable statistical properties. Perhaps, statistical properties have some deeper significance. The five independent measurements were then combined into one composite measurement. The statistical properties of the composite sets of measurements are given in Table 1. The table shows that mean increases linearly with bin size, which indicates that signal and background have constant strength. Variance is higher than the mean in all sets, which suggests that observed photocount distributions are not normal. Skewness is not zero, which implies skewed distribution of data points. Kurtosis and other moments (not shown in the table) are non-zero and large, which again rules out normal distribution of data points. This is true for both photon signals and background.

The absence of normal distribution rules out the origin of fluctuations from random disturbance. Photon signals probably have some amount of long time coherence. We do not know any classical mechanism for transfer of information needed for this coherence. It perhaps, emanates from non-classical transfer of information [17]. A more informative parameter indicating non-classical nature of a photon signal is Q value of the set of measurements. It is defined as

$$Q = [(\langle n^2 \rangle - \langle n \rangle^2)/\langle n \rangle] - 1,$$

where $\langle n^2 \rangle$ is the mean of the squares of the counts and $\langle n \rangle$ is the mean of counts in the distribution. The values of Q nearly equal to -1 occur in normal distribution and

Table 1
Statistical behavior of photon emission from background and three body sites at three bin sizes

Site	Bin size (ms)	Data points	Mean	Variance	Skewness	Kurtosis	Q	Fano factor
Background	50	20,000	0.29	0.90	6.3	58	2.05	1.05
Background	100	10,000	0.59	1.68	4.2	28	1.82	0.82
Background	200	5000	1.24	3.76	3.0	13	2.04	1.04
Leg	50	20,000	0.58	1.13	4.1	32	0.96	0.15
Leg	100	10,000	1.09	2.29	3.2	19	1.10	0.29
Leg	200	5000	2.27	4.78	2.0	6	1.10	0.30
Forehead	50	20,000	0.89	1.93	9.7	340	1.15	0.52
Forehead	100	10,000	1.70	3.21	3.1	26	0.88	0.53
Forehead	200	5000	3.27	5.99	1.7	5	0.84	0.49
Palm	50	20,000	1.60	2.36	2.2	13	0.47	0.53
Palm	100	10,000	3.09	4.59	1.6	6	0.49	0.65
Palm	200	5000	6.09	9.20	1.5	8	0.51	0.66

Mean, variance, kurtosis, skewness, Q and Fano factor and number of measurements in data sets derived after merging of data points from recordings obtained on one subject.

indicate a classical photon signal. The value $Q = 0$ occurs in Poisson distribution and indicates a quantum photon signal in coherent state. The values $Q > 0$ and $Q < 0$ occur, respectively, in super and sub Poisson distributions. Both indicate the possibility of a quantum photon signal in a squeezed state. It is pointed out that Q is a measure of the uncertainty in energy or amplitude of the associated electric field. $Q > 0$ implies large uncertainty in amplitude and hence less uncertainty in phase. The Q of the set of measurements in an ensemble of systems represented by a quantum state has a definite value and its values in different sets of measurements should lie in a small range. The measured values of Q in different quantum states should lie in different ranges. The behavior of the measured values of Q is a good indicator of the quantum nature and type of quantum state.

The Q and mean in five independent measurements at the three sites are plotted in Fig. 3. The values of Q and mean at five measurements are connected by lines for the sake of clarity. Both Q and the mean do not vary much in these measurements. The background has a higher value of Q but a lower value of the mean than the signal. The variation in Q is much more in different measurements in the background. The figure again shows an almost linear increase of mean with bin size. The value of Q does not change with bin size. The value of Q is nearly same in signals from leg and forehead and is slightly smaller in signals from palm. The measurements suggest that Q is a new measurable attribute of the subject.

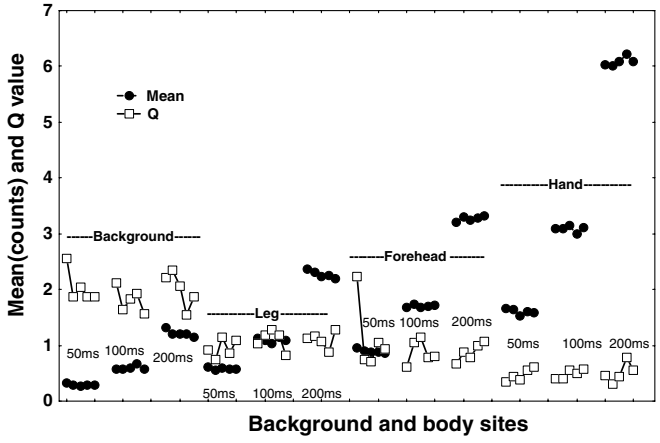

Fig. 3. Q value and mean of different sets of 4000 measurements: the body sites of measurements are indicated in the horizontal axis and bin size in the figure. The values in repeat measurements are connected by lines.

The calculated values of Q indicate a non-classical nature of background as well, which is an unexpected result. A substantial amount of background and its non-classical component make the usual procedure of obtaining properties of the signal by subtracting background contribution suspect. One needs a procedure that does not resort to background subtraction. We have suggested one such procedure [9]. The procedure is based on the assumption that a living system emits a low intensity photon signal in a quantum squeezed state specified by two complex parameters α and ξ, or equivalently by four real parameters $|\alpha|$, r, θ and ϕ. All measurable quantities of the signal can be calculated from its quantum state and are expressed in terms of four real parameters. The measurable quantities include average intensity and various probabilities of detecting photons. The calculations of average intensity and probabilities are straightforward and the calculated values are given in Ref. [18]. The four real parameters of the state, called squeezed state parameters henceforth, are estimated by least square minimization of the difference between calculated and observed probabilities. A function F of parameters is defined as the sum of the squares of difference between observed and calculated probabilities. F is a nonlinear function and has many local minima. Repeating the minimization procedure with different initial values of parameters identifies the true minimum. The value of the function at the true minimum $F_{\min}$ depends on the background noise and is an indicator of the goodness of fit. One expects $F_{\min}$ to be zero in the absence of noise. It is our contention that a random classical noise of moderate amount does not affect the estimated values of the parameters though it enhances the value of $F_{\min}$ and decreases the

sharpness of minimum. The presence of a non-classical component of the noise will, however, affect the estimated values parameters.

The squeezed state parameters were estimated in 60 sets of measurements (five independent measurements of 4 signals at 3 bin sizes). The four signals were background and at three body sites. The estimated parameters lacked robustness. The parameters for the background were quite different in repeat measurements and in measurements with different bin sizes. The values of $F_{\min}$ were also higher, so that fits were of poor quality, perhaps because a set of measurements had a small number of points and various probabilities were not correctly determined. Merging five repeat sets of measurements into a set partly rectified the error and it improved the determination of probabilities and enhanced the robustness of estimated parameters. The values of $F_{\min}$ decreased by more than an order of magnitude in the merged sets indicating a considerable improvement in the quality of fits. The minimization program gave reasonable estimates of $|\alpha|$ and r, but not of θ and ϕ. The function $F(|\alpha|, r, \theta, \phi)$ had many minima and its value in these minima is almost the same. It was possible to obtain an acceptable fit for any value of θ or ϕ; the minimization program estimated a pair (θ, ϕ) that depended upon the initial values fed in the programme. The arbitrariness in the estimate of θ and ϕ was removed by imposing the equality of calculated and observed average intensities. The equality implies negligible background and hence was not imposed initially. The equality, however, removed the arbitrariness in the estimates of θ and ϕ. The number of minima of F were reduced to one or two. The equality allowed to express $|\alpha|$ in terms of r and intensity and therefore, reduced the free parameters for estimation to three, namely r, θ and ϕ. The calculated parameters, mean, $|\alpha|$, $N_{\max}$ and $F_{\min}$ from photon signals emitted at three body sites and background are given in Table 2 for three bin sizes. The value of $|\alpha|$ is calculated from the mean and r and it is given for completeness. $N_{\max}$ is the number of different non-zero photon counts observed in measurements with a probability higher than 10^{-4}. Photon counts greater than $N_{\max}$ were observed in a few bins and these were ignored and the cut-off was imposed so as to save time in calculations. We did calculate the parameters without the cut-off in a few cases and found that the cut-off did not affect the estimated values of the parameters. $F_{\min}$ is the sum of the squares of the residual at $(N_{\max}+1)$ probability points. Table 2 shows that the variations of θ and ϕ with bin sizes (of 50, 100 and 200 ms) in the measurements of background are higher than in the measurements at body sites.

Since the squeezed state description requires same values of parameters at different bin sizes, the variation in the estimates of θ and ϕ indicates that the squeezed state description of signals emitted at the body sites is more appropriate than of the background. In the next stage, we imposed the restrictions that squeezed state parameters have the same values at three bin sizes. The calculated common parameters, $F_{\min}$ and the number of points contributing to $F_{\min}$ are given in Table 3. This table shows that $F_{\min}$ for the background signal is much higher than for signals at the body sites, which again indicates that the squeezed state description of body site signals is more appropriate. $F_{\min}$ is least for the signal emitted at the palm, which indicates

Table 2
Mean, $N_{\max}$, and estimated parameters $|\alpha|$, r, θ, ϕ and $F_{\min}$ of the assumed squeezed state of signal emitted by background and three body sites at three bin sizes

Site	Bin size (ms)	Mean	$N_{\max}$	$\lvert\alpha\rvert$	r	θ	ϕ	$F_{\min}$
Background	50	0.293	17	0.284	0.446	0.858	0.878	4.83×10^{-4}
Background	100	0.594	18	0.606	0.460	0.672	1.410	5.47×10^{-4}
Background	200	1.235	17	0.996	0.475	0.234	1.300	1.46×10^{-4}
Leg	50	0.578	17	0.702	0.289	0.680	1.340	2.23×10^{-4}
Leg	100	1.094	18	1.000	0.295	0.667	1.440	5.44×10^{-4}
Leg	200	2.273	19	1.470	0.343	0.669	1.420	9.81×10^{-4}
Forehead	50	0.894	23	0.908	0.261	0.676	1.360	2.51×10^{-4}
Forehead	100	1.703	22	1.280	0.261	0.676	1.360	4.31×10^{-4}
Forehead	200	3.266	21	1.770	0.370	0.683	1.320	5.04×10^{-4}
Palm	50	1.603	19	1.250	0.174	0.678	1.360	1.88×10^{-4}
Palm	100	3.088	22	1.740	0.260	0.693	1.230	1.88×10^{-4}
Palm	200	6.087	27	2.450	0.296	0.698	1.200	2.05×10^{-4}

Table 3
Estimated parameters r, θ, ϕ and $F_{\min}$ of the assumed squeezed state of signal common to all bin sizes emitted by three body sites, and background

Site	Points	r	θ	ϕ	$F_{\min}$
Background	55	0.366	0.350	1.408	0.008
Leg	56	0.300	0.355	1.240	0.003
Forehead	69	0.288	0.357	1.194	0.002
Palm	71	0.213	0.359	1.139	0.001
Leg + forehead + palm	196	0.269	0.364	1.219	0.009

The parameters of the squeezed state common at the three body site are also given. Points are the number of points used in the minimization.

that the background has least influence in the probabilities observed in the most intense signal. The parameters at three body sites were not much different. We, therefore, obtained parameters common to the three body sites. The common parameters, $F_{\min}$ and number of probabilities used in the minimization are also given in Table 3. The value of $F_{\min}$ indicates that the quality of the common fit is nearly the same as the quality of fits at specific body sites and is far superior to the quality of fit of the background signal. The squeezed state parameters appear specific to a subject and not to a body site. The fit of the background signal is not too bad, which indicates that background noise has some non-classicality, which may affect the estimation of parameters. The non-classicality in the background is usually attributed to filtering of low-level signals by a cut-off voltage used in the counting mechanism. Cut-off voltage also affects the signal and its various probabilities, which makes estimated parameters measuring system dependent. The measuring system dependence, hopefully, is not overwhelming and estimated parameters reflect the properties of the emitting systems. The parameters given in Tables 2 and 3 are specific to a measuring system. Even then, we could conclude that squeezed state parameters of the signal from different sites have subject specific commonality. We intend to use this commonality in identifying different subjects. The potential applications necessitate the development of a procedure for eliminating or at least minimizing the effect of background in the estimation of squeezed state parameters.

3.3. Effect of background noise and its minimization

Background noise considerably affects the determination of the properties of low intensity signals and no acceptable procedure exists for making correction for the background and for estimating its effect. We ignored the background in our estimates of the parameters because of the hope that the background merely enhances the value of $F_{\min}$ but does not appreciably alter the estimate of parameters. This hope was fulfilled in the estimate of parameters of signals emitted by samples of lichens, where we obtained consistent results. Since photon signals of body sites are much weaker than those of lichens, our hope may not be completely fulfilled. Background noise may influence the estimate of the parameters. Non-classicality of the background enhances this influence. One has to evolve strategies to minimize the effect of the background in various properties of a signal. The strategy in statistical moments is well established; one simply subtracts the statistical moment of the background from the observed statistical moment. The strategy is based on the independence of background noise and signal and can be employed to obtain background corrected values of intensity and Q. The strategy as such cannot be applied for obtaining a background correction to observed probability distributions. The strategy is employed in the definition of the Fano factor [7] that has been used in inferring non-classicality of a time varying photon signal. The Fano factor can also be used in inferring non-classicality of a time independent signal, where it is equal to the background corrected Q plus one. Table 1 gives the Fano factor and the uncorrected Q of various signals. The background corrected value of Q is obtained by subtracting one from the Fano factor. Both the Q and the Fano factor of a signal in measurements made with three bin sizes lie in a small band. The band of the Fano factor is bigger than the band of Q, probably because subtraction of background contribution enhances the error of the Fano factor. The bands of Q (and also of the Fano factor) in signals at different sites are close to each other and are far apart from its band in the background signal.

The existence of a band indicates the spread in the values of Q due to background noise. The spread is small, which suggests that the estimated squeezed state parameters will have only small variations. The small variations in the squeezed state parameters of signals emitted by different sites are also indicated by the closeness of their bands. The parameters of 12 measurements (signals from three body sites and the background measured with three bin sizes) are given in Table 2. The parameters of a signal determined from measurements at three bin sizes do not differ much; θ has nearly same value, ϕ varies only slightly and r shows a little larger variation. It is a desirable result because the bin size is only an artefact of the measuring procedure and should not affect the estimate of parameters of a signal. The observed variations in parameters are small and probably arise because of the background noise. It should be ignored. Therefore, the parameters of signals are obtained by fitting the observed probabilities at three bin sizes together. These parameters are given in Table 3. The quality of fits remained nearly unaltered. Another feature of Table 2 is that the squeezed state parameters of signals from the three body sites do not differ much. We, therefore, investigated the possibility of obtaining parameters common to the signals from the three body sites. These parameters are given in Table 3. The quality of fits to different signals having common parameters is not much different, suggesting that the parameters are specific to a subject and not to a body site. The signals with different intensities emitted at the three body sites have the same quantum description. We have also checked the possibility of obtaining parameters common to signals and the background. The checking did not yield acceptable fits, which indicates that the background is very different from the signal emitted at body sites.

The difference between background and signal is poignantly brought out by the graphics of calculated and observed photocount distributions. These are depicted in Fig. 4 for data sets of 200 ms. A broad peak is present in those signals but not in the background. Each data set contains 5000 data points so the probabilities are not so well determined. It is reflected in the larger value of $F_{\min}$ and slightly more deviations in observed and calculated values.

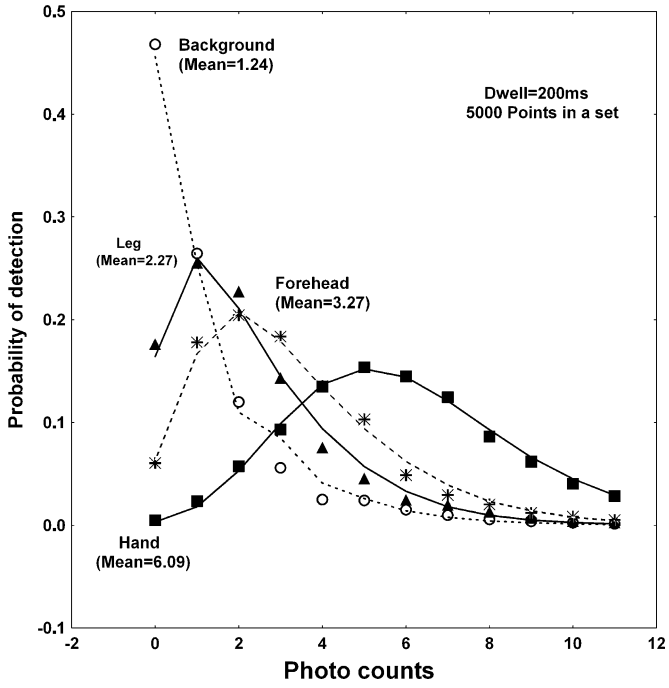

Fig. 4. Probability of photocount detection for bin size of 200 ms: the observed probabilities for background (○), leg (▲), forehead (✳) and palm (■) are plotted as symbols. The calculated probabilities in the assumed squeezed state are joined by lines. The figure also indicates the observed mean of the data sets.

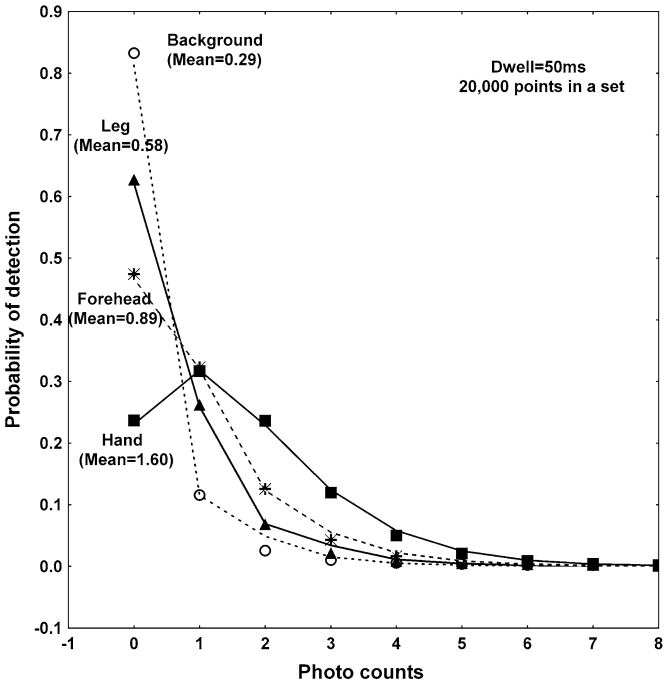

Fig. 5. Probability of photocount detection for bin size = 50 ms: the observed probabilities for background (○), leg (▲), forehead (✳) and palm (■) are plotted as symbols. The calculated probabilities in the assumed squeezed state are joined by lines. The figure also indicates the observed mean of the data sets.

The difference between background and signal is not so obvious in measurements with the bin size 50 ms depicted in Fig. 5. The peak is discernible only in the distribution of palm. The distribution of forehead and leg look similar to background. But there are some subtle differences, which the minimization program is able to identify. The program obtains values of parameters similar to values obtained from the data with bin size of 200 ms. The story of data sets with a bin size of 100 ms is similar. Here the peak is discernible in the distributions for the palm and forehead, but not for the leg.

The mean value of the background at bin size of 1 s is nearly equal to the mean value of the signal from the palm at the bin size of 200 ms. The observed distributions are depicted in Fig. 6. Both distributions have a broad peak but the two distributions are very different. The figure reiterates that the peaks of photocount distribution contain information that is deciphered by our analysis.

Figs. 4 and 5 also suggest the optimal bin size for detecting quantum features in photon signals emitted by the human body. The bin size of 200 ms appears most appropriate for palm. Any further increase of bin size will make the peak in distribution broader and difficult to detect. Similarly the optimal bin size should be 400 ms for measurements at the forehead and 600 ms for the leg. The mean value of the signal should be in the range 6–8 counts/bin. Finally the number of measurements in the set for determining probabilities should be more than 10,000 to obtain stable parameters.

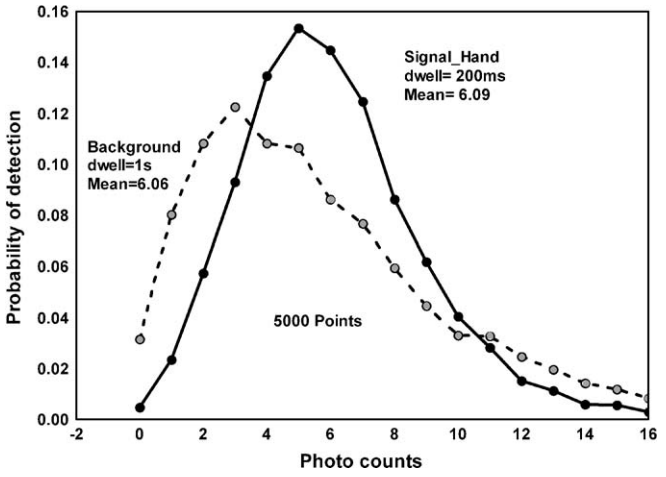

Fig. 6. Observed photocount distributions in a signal (■) and background (●) of almost identical intensities.

The determination of the squeezed state parameters was based on observed probabilities, which can be corrected for background contributions by assuming that the background and the signals are independent and uncorrelated. Let $P_{obs}(n)$ and $P_{bg}(n)$ be the measured probabilities of detecting n photons in signals from a body site and from the background for $n = 0, 1, 2, \ldots$. The correct probabilities $P_{cor}(n)$ for $n = 0, 1, 2, \ldots$ of detecting n photons of the signal are related to the observed probabilities by the following equations:

$$P_{obs}(0) = P_{cor}(0) \cdot P_{bg}(0)$$
$$P_{obs}(1) = P_{cor}(1) \cdot P_{bg}(0) + P_{cor}(0) \cdot P_{bg}(1)$$

The above equations express the fact that photon detection in a bin is a compound event made up of two independent components namely background and signal. No photon will be observed only if the observed photon number is zero in both components. One photon will be observed by two ways: one in the signal and zero in the background and zero in the signal, and one in the background. The equations can be written similarly for detecting any number of photons. The number of terms in the right hand side increases progressively. The above set of equations can be solved progressively to obtain $P_{cor}(n)$ starting from the first equation. The only problem in the procedure is the compounding of errors of both $P_{obs}(n)$ and $P_{bg}(n)$ up to n. As a result, the procedure breaks down after some n say n_0. Luckily, the probabilities for $n > n_0$ are very small and could be ignored. $P_{obs}(n)$ and $P_{cor}(n)$ are shown in Fig. 7 for a bin size of 200 ms. The two probabilities have similar behavior – the difference lies in the position of the peak that is shifted towards lower values in $P_{cor}(n)$. The parameters of the assumed squeezed state can again be calculated using $P_{cor}(n)$ and $Mean_{cor}$ obtained by subtracting the mean background from the observed mean. The calculated values are given in Table 4. The table shows a nearly zero value of r in signals from body sites. The only exception is the signal from forehead at 50 ms bin size, it has $r = 0.14$. The minima at different cases including the exceptional case of forehead are flat, so that $r = 0$ also gives reasonable fit in each case. The choice $r = 0$ makes θ and ϕ irrelevant and indeterminable as all probabilities are determined by $|\alpha|$ only. The choice implies that photons are emitted in a coherent state from three body sites and the distribution of probabilities is Poisson.

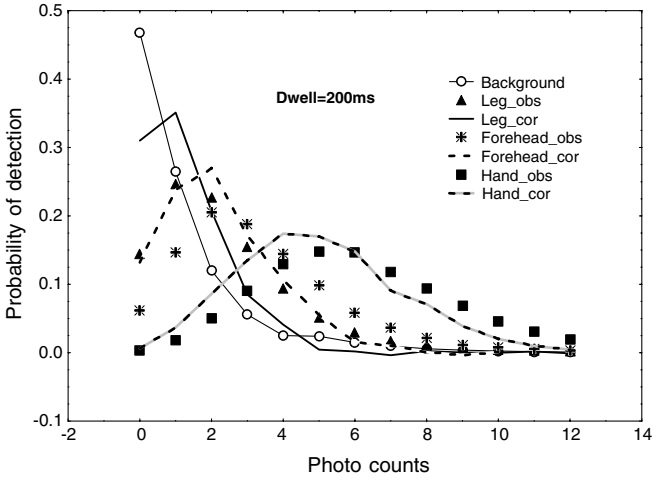

Fig. 7. Effect of background correction: the observed and corrected probabilities are given for background (○), leg (▲), forehead (✱) and palm (■) for bin size = 200 ms.

Our measurements and analysis are thus able to discover a structure in the fluctuating photon emission from human skin. The structure is measured through observed photocount distribution. The photocount distribution of a signal is different from that of background noise. The distributions can be expressed by analytic expressions involving three parameters. The parameters show nearly the same value in repeat measurements with different bin sizes. The parameters appear to have same values in measurements at three body sites. The parameters have, perhaps, same value at other locations of the body and are specific to a subject. The parameters may depend upon the measuring system and its noise. It is possible to correct the observed probabilities for background noise. The values of the parameters change considerably after the correction. The new values indicate that the quantum state of photon emitted by human skin could even be a coherent state in the subject being investigated.

Acknowledgements

The authors thank the Samueli Institute of Information Biology and the Bial Foundation for financial support; Zhonchen Yan for technical assistance, and Fritz-A. Popp, Yu Yan and John Ackerman for supportive suggestions.

Table 4
Estimated parameters $|\alpha|$, r, θ, ϕ and F_{min} of the assumed squeezed state of signal emitted by three body sites after correction for background probabilities

Site	Bin size (ms)	$Mean_{cor}$	N_{max}	$\lvert\alpha\rvert$	r	θ	ϕ	F_{min}
Leg	50	0.28	6	0.53	0.09	0.71	1.13	1.01×10^{-5}
Forehead	50	0.60	6	0.76	0.14	0.69	1.28	6.16×10^{-6}
Palm	50	1.31	7	1.14	0.04	0.56	1.85	5.57×10^{-5}
Leg	100	0.50	4	0.71	0.03	0.56	1.85	5.44×10^{-5}
Forehead	100	1.11	7	1.05	0.04	0.56	1.85	7.62×10^{-5}
Palm	100	2.49	9	1.58	0.08	0.60	1.17	1.42×10^{-4}
Leg	200	1.04	5	1.02	0.06	0.51	1.83	7.51×10^{-4}
Forehead	200	2.03	5	1.42	0.00	0.35	0.51	5.11×10^{-3}
Palm	200	4.85	11	2.20	0.00	0.17	0.09	6.75×10^{-4}
Background	50	0.29	17	0.28	0.45	0.86	0.88	4.83×10^{-4}
Background	100	0.59	18	0.61	0.46	0.67	1.41	5.47×10^{-4}
Background	200	1.24	17	1.00	0.48	0.23	1.30	1.46×10^{-3}

References

[1] V. Ntziachristos, J. Ripoll, L.V. Wang, R. Weissleder, Looking and listening to light: the evolution of whole-body photonic imaging, Nat. Biotechnol. 23 (2005) 313–320.

[2] R. Van Wijk, E.P.A. Van Wijk, An introduction to human biophoton emission, Forsch. Komplementärmed. Klass. Naturheilk. 12 (2005) 77–83.

[3] A. Boveris, E. Cadenas, R. Reiter, M. Filipkowski, Y. Nakase, B. Chance, Organ chemiluminescence: noninvasive assay for oxidative radical reactions, Proc. Natl. Acad. Sci. USA 77 (1980) 347–351.

[4] A. Boveris, E. Cadenas, B. Chance, Ultraweak chemiluminescence: a sensitive assay for oxidative radical reactions, Fed. Proc. 40 (1981) 195–198.

[5] H. Inaba, Super-high sensitivity systems for detection and spectral analysis of ultraweak photon emission from biological cells and tissues, Experientia 44 (1988) 550–559.

[6] R. Van Wijk, D.H.J. Schamhart, Regulatory aspects of low intensity photon emission, Experientia 44 (1988) 586–593.

[7] M. Kobayashi, B. Devaraj, H. Inaba, Observation of super-Poisson statistics of bacterial (*Photobacterium phosphoreum*) bioluminescence during the early stage of cell proliferation, Phys. Rev. E 57 (1998) 2129–2133.

[8] R.P. Bajpai, Quantum coherence of biophotons and living systems, Indian J. Exp. Biol. 41 (2003) 514–527.

[9] R.P. Bajpai, Biophoton emission in a squeezed state from a sample of *Parmelia tinctorum*, Phys. Lett. A 322 (2004) 131–136.

[10] R.P. Bajpai, Squeezed state description of the spectral decompositions of a biophoton signal, Phys. Lett. A 337 (2005) 265–273.

[11] M. Kobayashi, Modern technology on physical analysis of biophoton emission and its potential extracting the physiology information, in: F. Musumeci, L.S. Brizhik, M.W. Ho (Eds.), Energy and Information Transfer in Biological Systems, World Scientific, New Jersey, 2003, pp. 157–187.

[12] R. Van Wijk, M. Kobayashi, E.P.A. Van Wijk, Spatial characerization of human ultra-weak photon emission, in: L. Beloussiv, V.L. Voeiikov, V.S. Martynyuk (Eds.), Biophotons and Coherent Systems in Biology, Kluwer, New York, 2006 (in press).

[13] S. Cohen, F.A. Popp, Biophoton emission of the human body, J. Photochem. Photobiol. B 40 (1997) 187–189.

[14] E.P.A. Van Wijk, R. Van Wijk, Multi-site recording and spectral analysis of spontaneous photon emission from human body, Forsch. Komplementärmed. Klass. Naturheilk. 12 (2005) 96–106.

[15] R. Van Wijk, E.P.A. Wijk, Ultraweak photon emission of human body, in: S. Xun, R. Van Wijk (Eds.), Biophotonics – Optical Science and Engineering for the 21st Century, Springer, New York, 2005, pp. 173–184.

[16] R. Van Wijk, E.P.A. Van Wijk, Human biophoton emission, Recent Res. Devel. Photochem. Photobiol. 7 (2004) 139–173.

[17] H.P. Yuen, Two-photon coherent states of the radiation field, Phys. Rev. A 13 (1976) 2226–2243.

[18] M. Orszag, Quantum Optics, Springer, Berlin, Heidelberg, 2000, pp. 29–49.